Separation Science and Technology
Publication details, including instructions for authors and subscription information:
http://www.informaworld.com/smpp/title~content=t713708471

Principles and Applications of Gas Separation in Nonfrosting Technology

Tsair-Wang Chung[a]
[a] CHEMICAL ENGINEERING DEPARTMENT, CHUNG YUAN UNIVERSITY, CHUNGLI, TAIWAN, REPUBLIC OF CHINA

To cite this Article Chung, Tsair-Wang(1997) 'Principles and Applications of Gas Separation in Nonfrosting Technology', Separation Science and Technology, 32: 8, 1389 — 1402
To link to this Article: DOI: 10.1080/01496399708000967
URL: http://dx.doi.org/10.1080/01496399708000967

SEPARATION SCIENCE AND TECHNOLOGY, 32(8), pp. 1389–1402, 1997

Principles and Applications of Gas Separation in Nonfrosting Technology

TSAIR-WANG CHUNG
CHEMICAL ENGINEERING DEPARTMENT
CHUNG YUAN UNIVERSITY
CHUNGLI, TAIWAN 32023, REPUBLIC OF CHINA

ABSTRACT

Fan coils in low temperature storage rooms or freezing chambers are usually covered with frost during long-term operation. The fan coils can be installed sidewall or overhead in the freezing chamber, and the coils have cast aluminum fins. The usual solutions for frosting on the surfaces of freezing coils is to heat or spray with water to get rid of the frost periodically. However, these solutions are not only energy-consuming, but they also tends to spoil the refrigerated objects in the chamber. The main idea of this research is to achieve nonfrosting by using the technology of absorption-dehumidification to separate the water vapor from the circulating air in the freezing chamber during operations. Therefore, an experimental determination of nonfrosting technology using absorption principles was employed in this study. In the absorption-dehumidification device, the water vapor was absorbed into the liquid desiccant solution, and the diluted solution was regenerated by using the heat sources combined with waste heat from the freezing machine and major heat from a modified water heater. The dried air from the absorption-dehumidification device was circulated in the freezing chamber. The chamber operated at a temperature of -5 to -10°C. Since most of the water vapor in the circulating air is removed by the absorption-dehumidification device, less water vapor can be condensed on the coils. Therefore, no frosty coils were found in this freezing chamber during long-term operation.

INTRODUCTION

The operating conditions of freezing and refrigerating equipments are different in some ways, but their freezing circulation systems are similar. Generally speaking, freezing and refrigerating systems are closely akin to

air-conditioning systems. The only difference is the range of the operating temperature on the working fluid. Freezing and refrigerating systems require a temperature under 0°C, creating the phenomenon of frost on the surfaces of coils. Since the temperature on the surfaces of the coils goes under 0°C, which is lower than the dew point of the inlet air, the water vapor in the air will be separated and condensed on the surfaces of the coils. If the frost is thin, it will help the heat transfer of the coils. If the frost is too thick, it will, however, reduce the heat transfer on the surfaces of the coils. Moreover, as the frost becomes thicker, the airway becomes thinner, and the amount of entering air is decreased. Consequently, the freezing ability and suction pressure become lower, and the efficiency of the compressor is diminished. When the frost problem becomes worse, the surface of the fan becomes ice-frozen, and the fan will become stuck and burn the fan motor. This research trys to solve these problems by means of the absorption-dehumidification technique. This technique will not only make the freezing compressor durable, but also provides innovation in traditional nonfrosting technology.

Absorption-dehumidification devices are widely used in both industry and residences. Constant system performance during long-term operation is the most important factor for using this type of device. Maintaining the working solution concentration during operations can prevent system performance variation. Therefore, the development of a control technique for the solution concentration is necessary in order to apply these absorption-dehumidification devices for nonfreezing systems.

The mass transfer coefficient or the height of a transfer unit is the most important parameter in designing absorption-dehumidification devices. This parameter also provides a means of comparing system performance under different operating conditions. Grover et al. (1) compared, theoretically, the performance of two absorption systems: one employed water–lithium chloride as the desiccant and the other one used water–lithium bromide. According to them, lithium chloride solution is a better adsorbent because of its lower corrosivity and fewer health hazards. However, a water–lithium chloride solution has a higher viscosity than a water–lithium bromide solution of comparable concentration, which reduces the heat transfer rate in the system. Gandhidasan et al. (2) developed several correlations for heat and mass transfer coefficients for a packed tower that employed an aqueous calcium chloride solution and used ceramic Raschig rings and Berl saddles as packings. Their reasons for using calcium chloride was that it was the least expansive and most readily available. However, their correlations are only useful for designing water–calcium chloride systems. A more recent correlation was developed by Chung (3) for the dehumidification of air by an aqueous lithium

chloride solution. His correlation is a function of the properties of the liquid absorbent and packing material. Therefore, the correlation can be extended to other packed tower operations if the parameters are available. Chung's correlation was selected for designing the dehumidifier and regenerator used in this nonfrosting system. The aqueous lithium chloride solution was chosen as the liquid desiccant, and the Pall ring was used as the packing material in this study.

The performance of the absorption-dehumidification device in this nonfrosting system was evaluated under various operating conditions. The mass transfer coefficient and the height of a transfer unit of the absorption-dehumidification device in the system will also be calculated and compared to those in the open literature. The main sources of humidity are door-opening and the leakage in the freezing chamber (4). The determination of the nonfrosting ability in a system was conducted by observing the frost thickness on the freezing coils in every constant moment of door-opening during long-term operation.

EXPERIMENTAL

The block diagram of the nonfrosting system is shown in Fig. 1. The main components of this nonfrosting system include a freezing chamber, a liquid desiccant dehumidifier (or an absorber), a regenerator, a heat source for regeneration, and a freezing machine to decrease the liquid temperature in the dehumidifier. Except for the freezing chamber, the others are components of the absorption-dehumidification device. An absorption-dehumidification device combined with control units was successfully constructed in this study. The design of an "inverse U-shape" tunnel in the absorber and regenerator to allow air and the solution counterflow-contact increase the absorption rate and the regeneration rate. Also, in traditional absorbers, the carryover of the solution is a serious consideration. However, the "inverse U-shape" air tunnel with eliminators was used in the absorber and regenerator. Therefore, the carryover of the solution was neglected.

The flow diagram of the absorption-dehumidification device is shown in Fig. 2. The humidity of the circulating air in the chamber was measured by the hygrometer (accuracy: ± 0.2°C dew point, General Eastern, Model M4-RH). It maintained between 3 and 5 g water/kg dry air during the experimental runs. This moisture content is equivalent to conditions of 20–30°C and a relative humidity under 20%. The absorption system was capable of handling air velocities from 82 to 122 kg/m^2·min and liquid flow rates from 82 to 131 kg/m^2·min. These flow rates were calculated and reported as squared meters of cross-sectional area of the channel. Air

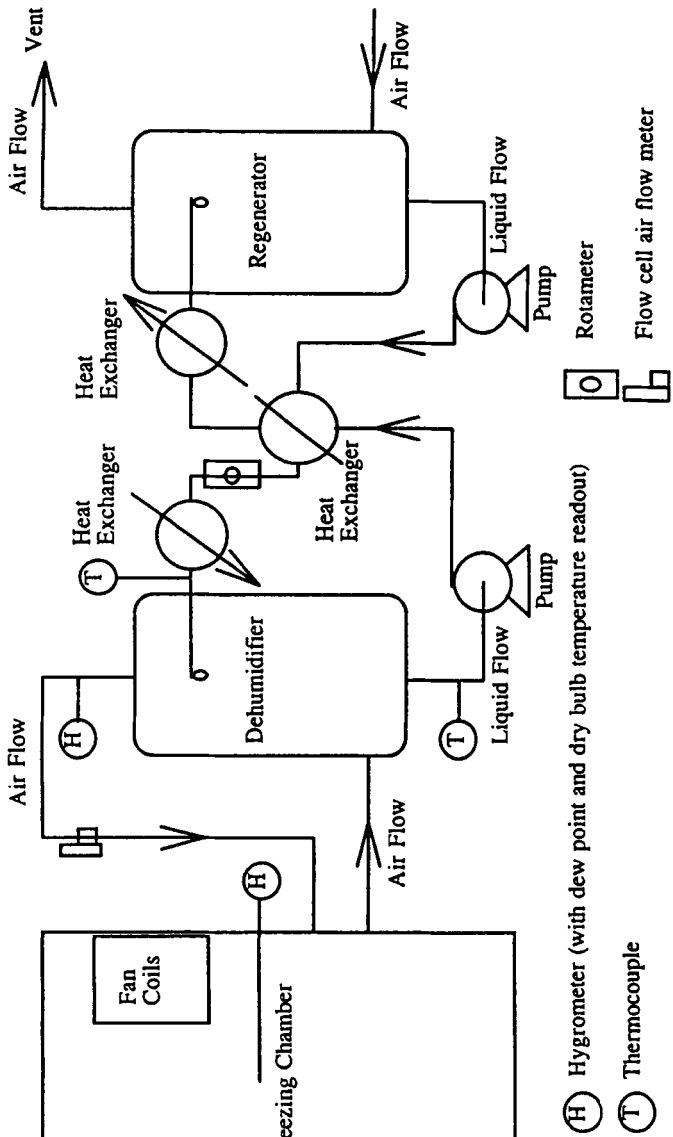

FIG. 1 The block diagram of the nonfrosting system.

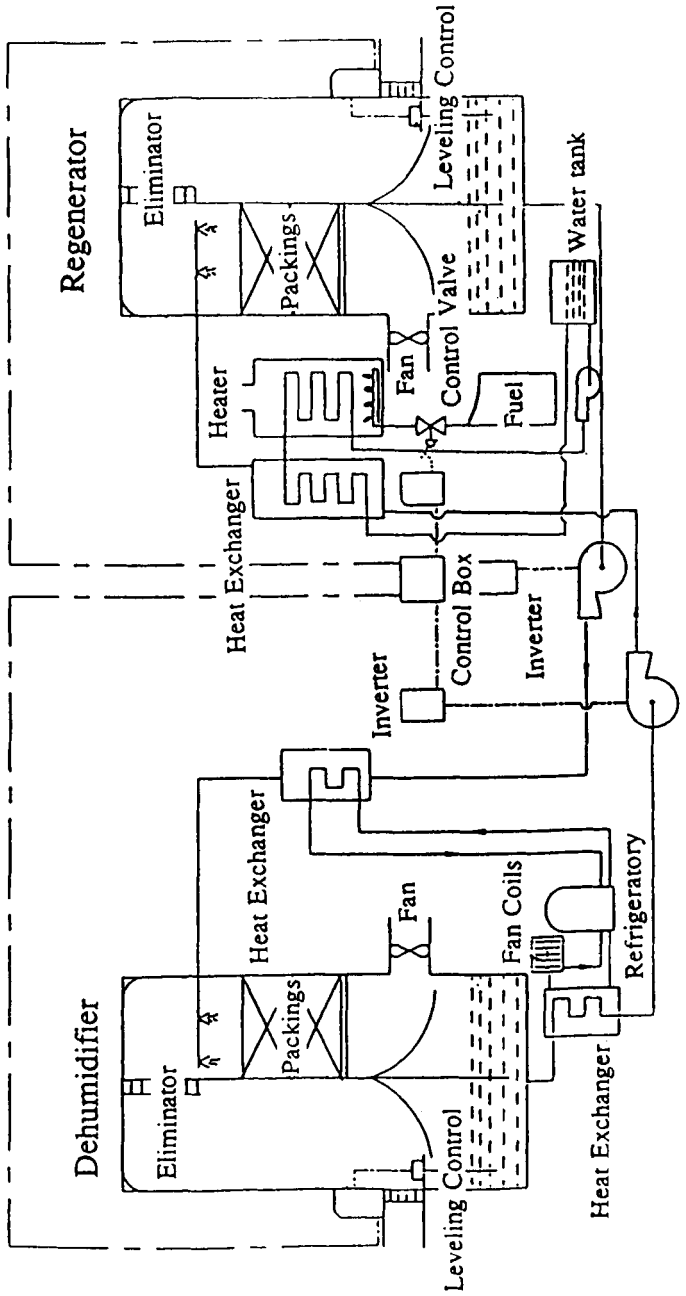

FIG. 2 The schematic flow diagram of the absorption-dehumidification device.

TABLE 1
Experimental Data of the Absorption-Dehumidification Device

No.	Air flow rate (kg/min)	Liquid flow rate (kg/min)	Liquid (LiCl) conc. (wt%)	Liquid inlet temp. (°C)	Liquid outlet temp. (°C)	Air inlet temp. (°C)	Air outlet temp. (°C)	Air inlet humidity (g water/ kg dry air)	Air outlet humidity (g water/ kg dry air)	Mass transfer coefficient (kmol/ $m^3 \cdot s$)	Height of transfer unit (m)
01[a]	15.0	10.0	40.0	15.0	21.0	27.5	26.5	15.0	8.8	0.17	0.43
02	15.0	12.0	40.0	15.0	21.0	26.0	26.2	15.0	8.8	0.17	0.43
03	15.0	14.0	40.0	15.0	22.0	25.0	26.0	14.8	8.8	0.16	0.43
04	15.0	16.0	40.0	15.0	22.0	26.5	26.4	15.0	8.7	0.17	0.42
05	10.5	10.0	40.0	15.0	19.0	29.0	26.6	14.8	9.2	0.10	0.49
06	12.0	10.0	40.0	15.0	20.0	29.5	26.2	15.2	9.4	0.12	0.49
07	13.5	10.0	40.0	15.0	20.0	28.5	26.3	14.5	8.8	0.14	0.46
08[a]	15.0	10.0	40.0	15.0	21.0	27.5	26.5	15.0	8.8	0.17	0.43
09	15.0	10.0	40.0	10.0	18.0	28.5	24.7	14.0	6.6	0.23	0.31
10[a]	15.0	10.0	40.0	15.0	21.0	27.5	26.5	15.0	8.8	0.17	0.43
11	15.0	10.0	40.0	20.0	24.0	28.5	28.2	14.0	9.2	0.14	0.52
12	15.0	10.0	40.0	25.0	28.0	28.5	30.2	14.0	9.8	0.13	0.55
13	15.0	10.0	42.5	15.0	24.0	30.0	28.6	15.0	8.2	0.19	0.37
14[a]	15.0	10.0	40.0	15.0	21.0	27.5	26.5	15.0	8.8	0.17	0.43
15	15.0	10.0	37.5	15.0	21.0	25.5	23.7	15.0	9.0	0.16	0.46

[a] Numbers 1, 8, 10, and 14 are the same test repeated in each parameter section for comparison.

TABLE 2a
Experimental Data of This Nonfrosting System[a] with a Door-Opening Time Interval of 0 min/h

Time	Solution inlet temperature in dehumidifier (°C)	Solution outlet temperature in dehumidifier (°C)	Atmospheric temperature (°C)	Atmospheric humidity (g/kg dry air)	Air inlet temperature in dehumidifier (°C)	Air inlet humidity in dehumidifier (g/kg dry air)	Air outlet temperature in dehumidifier (°C)	Air outlet humidity in dehumidifier (g/kg dry air)	Desiccant solution concentration (wt% LiCl)	Frost thickness on the freezing coils (mm)
9:40	13.0	16.0	21.5	14.2	19.0	6.4	18.5	5.1	42.0	~0
10:40	19.0	18.0	23.5	13.4	−2.0	3.4	16.0	3.2	42.0	~0
11:40	15.0	13.0	23.0	14.2	−2.5	2.8	12.5	1.7	42.3	~0
12:40	17.0	14.0	23.0	13.7	−2.0	3.2	13.5	2.7	42.5	~0
13:40	13.0	12.0	22.5	13.2	0.0	2.6	12.0	2.0	42.5	~0
14:40	12.0	10.0	22.5	13.2	−1.0	2.8	11.0	2.2	42.3	~0
15:40	13.0	11.0	22.0	13.5	−3.5	2.7	11.0	2.6	42.0	~0
16:40	13.0	12.0	22.5	13.2	−3.5	3.0	7.5	2.4	42.0	~0

[a] Air flow rate: 15 kg/min. Liquid flow rate: 15 kg/min. Temperature of freezing chamber: −5°C.

TABLE 2b
Experimental Data of This Nonfrosting System[a] with a Door-Opening Time Interval of 0.5 min/h

Time	Solution inlet temperature in dehumidifier (°C)	Solution outlet temperature in dehumidifier (°C)	Atmospheric temperature (°C)	Atmospheric humidity (g/kg dry air)	Air inlet temperature in dehumidifier (°C)	Air inlet humidity in dehumidifier (g/kg dry air)	Air outlet temperature in dehumidifier (°C)	Air outlet humidity in dehumidifier (g/kg dry air)	Desiccant solution concentration (wt% LiCl)	Frost thickness on the freezing coils (mm)
10:30	17.0	17.0	20.5	10.2	4.5	2.0	4.5	2.0	42.5	~0
11:30	9.0	8.0	22.0	11.0	0.5	2.3	10.0	2.1	42.5	~0
12:30	17.0	13.0	22.5	10.5	−5.0	2.4	12.0	2.0	42.5	~0
13:30	14.0	13.0	23.0	10.2	−1.0	2.8	9.0	2.3	43.0	~0
14:30	14.0	12.0	23.5	11.2	−3.5	2.7	9.0	2.3	43.0	~0
15:30	16.0	11.0	23.5	11.2	1.0	2.1	11.0	2.1	44.0	~0
16:30	12.0	10.0	23.0	11.0	−2.5	3.0	8.0	2.7	43.5	~0

[a] Air flow rate: 15 kg/min. Liquid flow rate: 15 kg/min. Temperature of freezing chamber: −5°C.

TABLE 2c
Experimental Data of This Nonfrosting System[a] with a Door-Opening Time Interval of 1.0 min/h

Time	Solution inlet temperature in dehumidifier (°C)	Solution outlet temperature in dehumidifier (°C)	Atmospheric temperature (°C)	Atmospheric humidity (g/kg dry air)	Air inlet temperature in dehumidifier (°C)	Air inlet humidity in dehumidifier (g/kg dry air)	Air outlet temperature in dehumidifier (°C)	Air outlet humidity in dehumidifier (g/kg dry air)	Desiccant solution concentration (wt% LiCl)	Frost thickness on the freezing coils (mm)
9:30	9.0	14.0	21.5	13.5	19.5	7.9	21.5	7.5	44.0	~0
10:30	9.0	9.0	24.5	12.8	−0.5	3.7	8.5	2.5	43.0	~0
11:30	11.0	9.0	26.0	14.4	2.0	1.9	6.5	1.8	44.0	~0
12:30	9.0	9.0	26.5	12.8	4.0	3.7	8.5	1.8	44.0	~0
13:30	10.0	10.0	28.0	14.2	−1.0	2.3	12.0	1.9	44.0	~0
14:30	11.0	10.0	28.5	14.0	2.0	2.0	10.5	2.0	44.0	~0
15:30	6.0	8.0	28.5	14.8	0.0	2.5	9.5	1.7	44.0	~0

[a] Air flow rate: 15 kg/min. Liquid flow rate: 15 kg/min. Temperature of freezing chamber: −5°C.

TABLE 2d
Experimental Data of This Nonfrosting System[a] with a Door-Opening Time Interval of 2.0 min/h

Time	Solution inlet temperature in dehumidifier (°C)	Solution outlet temperature in dehumidifier (°C)	Atmospheric temperature (°C)	Atmospheric humidity (g/kg dry air)	Air inlet temperature in dehumidifier (°C)	Air inlet humidity in dehumidifier (g/kg dry air)	Air outlet temperature in dehumidifier (°C)	Air outlet humidity in dehumidifier (g/kg dry air)	Desiccant solution concentration (wt % LiCl)	Frost thickness on the freezing coils (mm)
9:30	8.0	22.0	26.0	18.2	8.0	5.0	22.0	6.0	40.0	~0
10:30	17.0	12.0	25.5	17.0	−3.5	3.0	14.0	2.6	40.0	~0
11:30	19.0	14.0	25.5	17.0	−6.5	2.1	16.0	2.4	40.0	~0
12:30	14.0	13.0	30.0	24.5	−7.0	2.0	14.0	2.1	40.0	~0
13:30	19.0	13.0	29.0	17.8	2.5	2.3	10.5	2.0	40.5	~0
14:30	16.0	14.0	29.0	17.8	−7.5	1.8	14.5	2.0	41.0	~0
15:30	17.0	14.0	28.0	17.3	−3.0	2.9	12.0	2.2	41.0	~0
16:30	15.0	13.0	27.5	16.7	−1.0	3.5	11.5	2.0	41.0	~0

[a] Air flow rate: 15 kg/min. Liquid flow rate: 15 kg/min. Temperature of freezing chamber: −10°C.

TABLE 2e
Experimental Data of This Nonfrosting System[a] with a Door-Opening Time Interval of 3.0 min/h

Time	Solution inlet temperature in dehumidifier (°C)	Solution outlet temperature in dehumidifier (°C)	Atmospheric temperature (°C)	Atmospheric humidity (g/kg dry air)	Air inlet temperature in dehumidifier (°C)	Air inlet humidity in dehumidifier (g/kg dry air)	Air outlet temperature in dehumidifier (°C)	Air outlet humidity in dehumidifier (g/kg dry air)	Desiccant solution concentration (wt% LiCl)	Frost thickness on the freezing coils (mm)
9:30	14.0	14.0	29.5	17.5	3.0	4.0	17.0	3.0	40.0	~0
10:30	17.0	15.0	29.5	17.5	−2.0	3.2	17.5	3.1	40.0	~0
11:30	16.0	14.0	30.5	17.9	−2.0	3.2	15.0	2.1	40.0	~0
12:30	15.0	14.0	28.5	17.9	−7.0	2.0	16.5	3.1	40.0	~0
13:30	20.0	14.0	28.5	18.0	−7.0	2.0	14.5	2.2	40.0	~0
14:30	18.0	15.0	29.5	18.4	−8.0	1.8	16.0	2.9	40.0	~0
15:30	18.0	15.0	29.0	18.6	−7.0	2.0	15.0	3.0	40.0	~1
16:30	17.0	14.0	29.0	18.6	−7.0	2.0	14.5	2.8	40.0	~1

[a] Air flow rate: 15 kg/min. Liquid flow rate: 15 kg/min. Temperature of freezing chamber: −10°C.

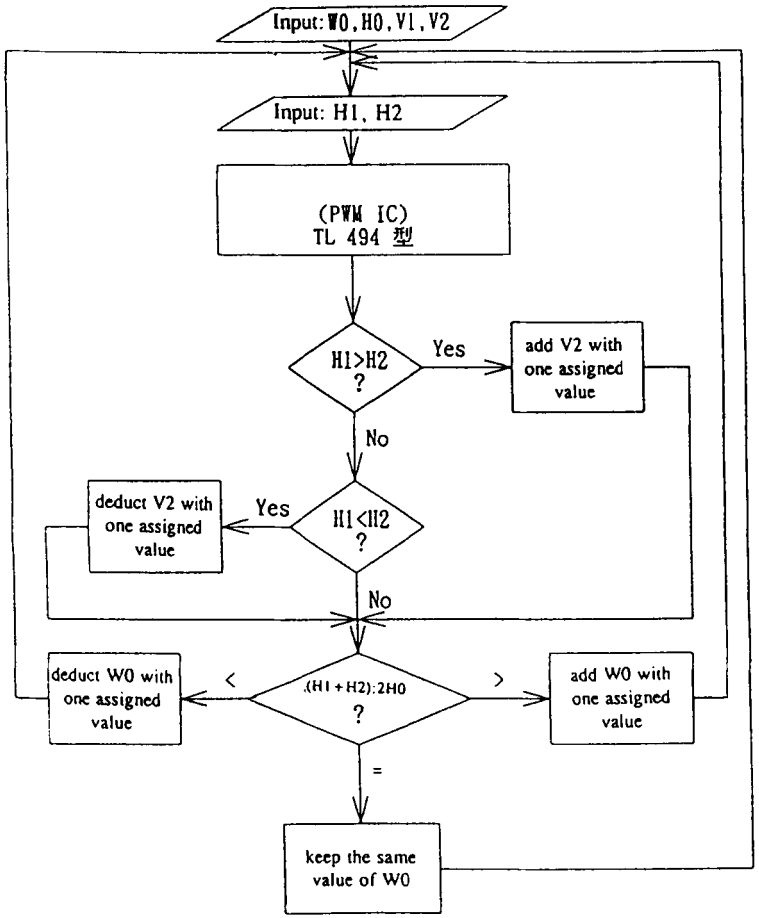

Solution level in the dehumidifier: H1
Solution level in the regenerator: H2
Balance level of solution in the dehumidifier and regenerator: H0
Opening of the control valve for controlling the rate of fuel into the heater: W0
Motor for sending solution into the dehumidifier: Motor1
Motor for sending solution into the regenerator: Motor2
Speed of Motor1 : V1
Speed of Motor2 : V2

FIG. 3 The control algorithm of the absorption-dehumidification device.

flow rates were measured by using the flow cell, and liquid flow rates were measured by using the rotameter. Aqueous desiccant solutions that contained from 37.5 to 42.5% weight of lithium chloride were used in this study. Testing of the concerned components of the system was maintained during this research project. Tables 1 and 2a–e show the different parameters measured in this study.

Automatic control of the solution concentration was designed and tested in this study. Since the concentration of the desiccant solution was kept constant, the system could be operated smoothly during long-term operation. The flow chart of this control algorithm is shown in Fig. 3. Signals of different levels from the absorber and the regenerator are sent to the control box, which contains a pulse width modulation (PWM) controller for controlling solution levels in the dehumidifier and the regenerator. The motor speeds of the solution pumps are changed by the inverters, and the inverters are also controlled by the control box. The solution regeneration rate is varied with the temperature of solution into the regenerator, and the temperature of solution into the regenerator is controlled by the valve opening of the fuel into the water heater. The electric valve of the fuel is also controlled by the control box. Therefore, the solution levels of the dehumidifier and regenerator can be used to control the solution flow rates and regeneration rates to keep the level balance and the concentration constant by using the PWM controller.

The absorption-dehumidification device, combined with a freezing chamber, was constructed to be a nonfrosting freezing chamber. Since almost no frost was seen during the experimental runs, visual monitoring was used to measure the frost thickness. Also, the frost thickness was observed in every constant moment of door-opening for each experimental run.

RESULTS AND DISCUSSION

The performance of the absorption-dehumidification device was evaluated by carrying out a series of experimental runs. The parameters that were varied during the experimentation included air flow rate, liquid concentration and flow rate, temperature, and humidity. The operating conditions are presented in Table 1. The overall mass transfer coefficient is derived following the procedure given by Hines and Maddox (5). The molar flux in this system is written as the product of an overall mass transfer coefficient and the difference between the bulk and equilibrium concentration as

$$N_A = \frac{d(Gy_A)}{adZ} = \frac{K_{GA}}{\beta_{v-v^*}}(y - y_A^*) \tag{1}$$

where G is the molar flow rate of air, and the bulk flow concentration factor for transfer through a stagnant film is given by

$$\beta_{v-v^*} = (1 - y_A)_{*M} = \frac{(1 - y_A^*) - (1 - y_A)}{\ln\left(\frac{1 - y_A^*}{1 - y_A}\right)} = \frac{y_A - y_A^*}{\ln\left(\frac{1 - y_A^*}{1 - y_A}\right)} \tag{2}$$

By rearranging Eqs. (1) and (2) and integrating, the overall mass transfer coefficient can be written as

$$(K_{GA}a)_{avg} = \frac{G}{Z}\int_{y_{A,a}}^{y_{A,b}} \frac{(1 - y_A)_{*M}}{(1 - y_A)} \frac{dy_A}{(y_A - y_A^*)} \tag{3}$$

Most experimental data on packed-bed absorber are generally given in height of a transfer unit (HTU) rather than in terms of the mass transfer coefficient. The HTU is less dependent on the liquid or gas flow rate. Therefore, it provides a means of comparing the efficiency of various packings. The HTU is defined as the molar velocity based on total column cross-section divided by the overall mass transfer coefficient.

$$H_{OG} = \frac{G}{K_{GA}a} \tag{4}$$

The higher the overall mass transfer coefficient is, the lower the height of a transfer unit will be.

The performance testing of the dehumidifier under the atmospheric conditions is shown in Table 1. The liquid flow rate used in the absorber was significantly larger than the minimum liquid flow rate determined from the equilibrium calculation (6). Therefore, the liquid flow rate, as varied in Table 1 (No. 1 to No. 4), does not appear to have a significant effect on the overall mass transfer coefficient. However, an increase in the overall mass transfer coefficient with increasing air flow rate is shown in Table 1 (No. 5 to No. 8). The mass transfer coefficient varied linearly with the inlet air flow rate. In Table 1 (No. 9 to No. 12), there was an increase in the overall mass transfer coefficient with decreasing liquid inlet temperature. This is because the maximum possible moisture removal by the liquid desiccant under a given operating condition is determined by the temperature of the desiccant solution in the absorber. As expected, mass transfer coefficients were greater for the 42.5 wt% lithium chloride solution than for the 37.5 wt% solution. In Table 1 (No. 13 to No. 15), the overall mass transfer coefficients were varied with the liquid concentrations. The

values of the mass transfer coefficients obtained in this study using polypropylene Pall rings were higher than those reported by Scalabrin and Scaltriti (7), who used glass Raschig rings and polypropylene Pall rings. This is because the gas–liquid flow ratios in the study of Scalabrin and Scaltriti were not of the proper design. However, the values of the mass transfer coefficients obtained in this study were in the same order of magnitude with those reported by Gandhidasan et al. (8) and Lof et al. (9).

In the case of a 18,750 ft^2 warehouse in Chicago, IL, USA, the source of humidity was mainly due to the number of times the door was opened and the leakage (4). Therefore, experiments observing frost-formation for door-opening intervals of 0, 0.5, 1, 2, and 3 min/h were used in this -5 to -10°C freezing chamber. The frost thickness was observed at the beginning of each door-opening during the experimental run. When the temperature of the freezing chamber was set at -5°C and the door was closed, the humidity of the circulation air could be pulled down from 13–14 to 2–3 g water/kg dry air. The latent load (or humidity) was limited because all the air was returned and the door was closed. Therefore, the system could reach equilibrium conditions quickly, and there was almost no frost on the freezing coils. When the temperatures of the freezing chamber were set at -5 to -10°C and the time interval of door-opening were set at 0.5 to 3.0 min/h, the latent load in the chamber increased tremendously. However, the system can still pull down the air humidity to 2–3 g water/kg dry air easily. By the way, only an approximate 0.1 mm thickness of frost was found on the shaft of the fan motor because of the bad circulation in this area. After a long period of operating time, the frost on the shaft no longer increased. Tables 2a–e show that almost no frost was found on the freezing coils in all experimental runs.

CONCLUSION

Under the operating conditions tested on the absorber, the height of a transfer unit calculated from the mass transfer coefficient was significantly affected by the liquid temperature and concentration.

This nonfrosting freezing chamber can be operated smoothly under automatic control of the solution concentration. It has high stability and no frosty coils during long-term operation. The absorption-dehumidification device removed water vapor from the circulating air in the freezing chamber and reduced the opportunity for frost to condense on the freezing coils. Therefore, defrosting of the freezing system is no longer necessary.

The design of an automatic control for the solution concentration is another important feature of this system. The control unit has advantages of low cost, easy setup, and high stability in comparison with commercial units.

NOMENCLATURE

a	specific interfacial surface for contact of a gas with liquid (m^2/m^3)
G	superficial mass velocity of air ($kmol/m^2 \cdot s$)
K_{GA}	overall gas phase mass transfer coefficient ($kmol/m^2 \cdot s$)
N_A	flux of species A at the interface ($kmol/m^2 \cdot s$)
y_A	mole fraction of water vapor in the bulk phase (kmol/kmol gas mixture)
$y_{A,a}$	mole fraction of water vapor in the outlet air of absorber (kmol/kmol gas mixture)
$y_{A,b}$	mole fraction of water vapor in the inlet air of absorber (kmol/kmol gas mixture)
y_A^*	equilibrium mole fraction of water vapor in the air (kmol/kmol gas mixture)
Z	height of packing (m)
H_{OG}	height of a transfer unit (m)

REFERENCES

1. G. S. Grover, S. Devotta, and A. F. Holland, *Ind. Eng. Chem. Res.*, *28*(2), 250 (1989).
2. P. Gandhidasan, C. F. Kettleborough, and M. R. Ullah, *ASME J. Sol. Energy Eng.* *108*, 123 (1986).
3. T.-W. Chung, T. K. Ghosh, and A. L. Hines, Presentation at AIChE Topic Conference—Separation Technology, Miami Beach, FL, November 1–6, 1992.
4. L. G. Harriman III, *The Dehumidification Handbook*, Ch. 5, Munters Cargocaire Co., Amesbury, MA, 1990.
5. A. L. Hines and R. N. Maddox, *Mass Transfer Fundamentals and Applications*, Ch. 12, Prentice-Hall, Inc., Englewood Cliffs, NJ, 1985.
6. T.-W. Chung, T. K. Ghosh, and A. L. Hines, *Sep. Sci. Technol.*, *28*(1–3), 533 (1993).
7. G. Scalabrin and G. Scaltriti, *Termotecnica*, *38*(11), 65 (1984).
8. P. Gandhidasan and S. Satcunanathan, *Proceedings Biennial Congress International Solar Energy Society, 8th Meeting*, *3*, 1726 (1983).
9. G. O. G. Lof, T. G. Lenz, and S. Rao, *J. Sol. Energy Eng.*, *106*, 387 (1984).

Received by editor May 10, 1996
Revision received October 9, 1996